ANALYSIS AND DESIGN OF HYSTERETIC STRUCTURES FOR PROBABILISTIC SEISMIC RESISTANCE

by

D. Veneziano[I]

SYNOPSIS

A simple bilinear hysteretic system (Fig. 1) is located in a seismic area for a finite period of time. At the site, independent stationary earthquake motions occur according to a Poisson process; they have random duration and intensity but the same normalized spectral density. The expected ductility factor and the probability of failure at the end of the period are estimated through an approximate analytic model, which uses concepts of Random Vibration and Markov Theories; the analysis is extended to structures with initial damage and limited ductility. The approach is particularly attractive for design problems, when the system has to satisfy minimum performance requirements under stochastic dynamic actions.

INTRODUCTION

Hysteretic properties of elasto-plastic systems have a large - often beneficial - influence on the response to strong earthquakes. This happens at the expense of permanent deformations, and indeed the ductility factor must be considered as an index of damage.

For these systems the process of damage accumulation through plastic deformation has been studied extensively, but only in recent years, and limitedly to white noise, results have become available for the case of stochastic input[1,2]. The mathematical difficulties increase considerably if the structure does not fit the elasto-plastic model, or if the ground motions have nonconstant spectral density and random occurrence times. Finally, the analysis of damage in this stochastic environment could be viewed, at least theoretically, as a preliminary step towards systems design.

In this study, an approximate procedure is proposed for simple bilinear hysteretic systems with negative second stiffness. The model, which in the limit covers the elasto-plastic case, might result from geometric nonlinearity associated with gravity loads (Fig. 1) or from degrading material properties after yielding.

Two approaches have been developed so far for analyzing the stochastic accumulation of permanent deformation in systems of this type: one[3], which pioneered the problem, makes use of simulation methods; the other[4] suggests an analytic way, based on Random Vibration Theory. When the judgement of safety relies on the occurrence of rare events - such as collapse for seismic action - simulation becomes an expensive technique, and simplified analytic models, when feasible, should be preferred. The

[I]Assistente presso l'Instituto di Scienza delle Costruzioni, Facoltà di Ingegneria, L'Aquila, Italy.

expected progression of permanent deformation and the probability of failure (defined as reaching either of points A in Fig. 1) was studied earlier[5] on five bilinear systems excited by white noise. The following two paragraphs extend these results to any bilinear system with negative second slope, to any acceleration spectral density, to the case of damaged initial conditions and to the definition of failure as exceeding of a limit ductility factor. The last section contains examples of analysis and design problems; since the writer feels the importance of checking the accuracy of the present treatment via different methods, the stress is on potential applications, more than on technical results; nevertheless, interesting qualitative features emerge, as summarized in the conclusions.

THE EXPECTED NUMBER OF CYCLES TO FAILURE

The present paragraph focuses on the approximate computation of the expected number of cycles to failure, n_f ("cycle" stands for "natural period"), when collapse occurs at either of points A in Fig. 1. A more general definition of failure is introduced in the next paragraph, where n_f is used to compute important response statistics.

Let X denote the actual displacement of the mass relative to the ground, $\bar{X}$ be the static (or permanent) deformation, and $Y_S(\bar{X})$, $Y_I(\bar{X})$ be the plastic barrier levels, defined as the positive and negative values of $(X-\bar{X})$ corresponding to yielding (Fig. 2). $\bar{X}_M$ is the permanent deformation at failure. Starting with the undeformed system, after the first yielding has taken place the plastic barriers are no longer symmetric. As time goes on, inelastic deformations occur more and more frequently in the direction of the nearest barrier until eventually the static unstable condition is reached. An hypothetical deformation history is sketched in Fig. 3. The main assumption made at this stage was the stationarity of the response during the "elastic intervals" (Z=0 in Fig. 3b), which allowed one to construct a Markov model for describing how $\bar{X}$ evolves with time[5]. In general, the expected number of cycles to failure depends on all the input and system characteristics, but the examination of the numerical results in Ref. 5 has filtered out the importance of three quantities:

- r - the initial barrier level $y_s(0) = y_0$ normalized with respect to the r.m.s. of the stationary relative displacement in the "associated" elastic system (see Fig. 2);
- η - the ratio between the hysteretic energy to failure and the expected kinetic energy at first yielding;
- n_c - the mean time lag (expressed in cycles) between subsequent yieldings, when the system is still undeformed.

In terms of these quantities, n_f was approximated by a relation of the type[6]:

$$n_f = \eta \cdot n_c \cdot g(r,\eta) \ . \qquad (1)$$

Since the shape of the input spectral density has little effect on $g(r,\eta)$, this factor was estimated from the numerical results in Ref. 5.

It remains to be seen how to compute r, η and n_c. The treatment for

white noise being simpler, it is considered first. Let G_I denote the constant input spectral density. r, η and n_c further depend on the following system parameters: the natural frequency ω_n, the ratio of critical damping β, the initial barrier level y_0, and the stiffnesses K_1 and K_2 of the bilinear force-displacement relation:

$$r = y_0 \left\{ \frac{4\beta\omega_n^3}{\pi G_I} \right\}^{1/2} , \tag{2}$$

$$\eta = \frac{y_0^2 K_1^2}{|K_2| mE[\dot{x}^2],r} = \frac{K_1}{|K_2|} \frac{\omega_n^2}{E[\dot{x}^2],r} , \tag{3}$$

$$n_c = \frac{\nu_0}{n_r E[N^P],r} ; \tag{4}$$

where: m is the mass of the system; $E[\dot{x}^2],r$ is the second moment of the relative velocity when a plastic barrier is reached at level r; ν_0 is the mean rate of zero upcrossings in the associated elastic system; n_r is the expected rate of plastic clumps for symmetric barriers with normalized distance r; $E[N^P],r$ is the expected plastic clump size for the system with no initial deformation.

An interesting and practically important feature (see Ref. 6) is that n_f, introduced as a function of all the input-system parameters, is sensitive only to three quantities, namely r, β, $K_1/|K_2|$. Figure 4 contains plots of n_f versus r, for stiffness ratios ranging from 5 to 100, and 3% of critical damping. Results in the same form were obtained for other values of β[6]. The high sensitivity of n_f to the stiffness ratio comes from the assumption of unlimited ductility and decreases for relatively brittle systems (see next paragraph).

Actual ground motions typically show a non-constant spectral density in the frequency range of structural interest. The variability of the energy distribution has been often by-passed using an "equivalent" white noise. However, even if the r.m.s. of the relative displacement can be reproduced by a suitable choice of G_I, other characteristics of the response may differ considerably. In the evaluation of the expected number of cycles to failure for a nonconstant input spectral density, one has to consider, as additional variable, the natural frequency of the system; equations 1, 3 and 4 still hold, while Eq. 2 takes the more general form:

$$r = \frac{y_0}{I \left\{ \int_0^\infty |H(\omega)|^2 \, G_N(\omega) d\omega \right\}^{1/2}} \tag{5}$$

where: $H(\omega)$ is the transfer function from support acceleration to relative displacement; I^2 is the variance of the ground acceleration; and $G_N(\omega) = G(\omega)/I^2$ is the normalized input spectral density.

The expected number of cycles to failure was tabulated in Ref. 6 for the Kanai-Tajimi spectral density:

$$G(\omega) \propto \frac{1 + 4b^2\frac{\omega^2}{c^2}}{(1 - \frac{\omega^2}{c^2})^2 + 4b^2\frac{\omega^2}{c^2}} \quad , \text{ with: } \quad b^2 = 0.410, \; c^2 = 242 \; , \qquad (6)$$

and the following parameter ranges:

$$\omega_n = \pi \div 10\pi \quad , \qquad r = 0.2 \div 3.0 \quad ,$$

$$\beta = 0.01 \div 0.20 \quad , \quad K_1/|K_2| = 3 \div 100 \quad .$$

The effect of the energy distribution can be measured giving specific values to r, β, $K_1/|K_2|$ and computing the ratio n_f/n_{f_c} between the expected number of cycles to failure for the non-constant and constant spectral densities, as a function of the system natural frequency. In Fig. 5 this ratio is plotted for r = 1.00 and some representative values of β and $K_1/|K_2|$. The general shape of these curves closely resembles the non-constant spectral density to which they refer, indicating that;

- the white noise approximation is acceptable for very soft structures;
- n_f differs considerably from n_{f_c} for higher and more usual natural frequencies, reaching a maximum in the vicinity of the maximum input energy density;
- the "equivalent" white noise becomes an unconservative approximation for very stiff structures.

These variations are explained by the different frequency content of the elastic stationary response.

THE EXPECTED DUCTILITY FACTOR AND THE PROBABILITY OF FAILURE

In computing the expected number of cycles to failure we supposed the base motion to have infinite duration. In order to make any statement on the reliability of the system we also need the "equivalent" response duration with stationary properties during the elastic intervals, T. In the present paragraph, simple charts are presented which relate the expected permanent deformation and the probability of failure directly, although approximately, to n_f and to the number of response cycles; $N = T\nu_0$.

If the system has experienced at least one barrier impact and the actual permanent deformation was never exceeded before, the ductility factor μ is a linear function of $|\bar{X}|$:

$$\mu = 1 + \frac{|\bar{X}|}{\bar{X}_M} \frac{K_1}{|K_2|}$$

In Ref. 5, the expected permanent deformation was numerically computed for many values of N and for many excitation intensities. When n_f is fixed,

the plots of $E[|\bar{X}|]/\bar{X}_M$ versus N/n_f almost coincide for all the structures considered. Average curves[6] were used to get the chart in Fig. 6, which essentially relates n_f and N to the expected permanent deformation. From this chart one may extract several important pieces of information on the system performance.

(i) The expected number of cycles to failure for initially unsymmetric barriers, n_f'.

This condition may arise from an initial permanent deformation $\bar{X}_i$, from an horizontal permanent load F_i (see Fig. 1), or from a combination of the two. Figure 6 is used as follows. Define a parameter of "initial damage": $\bar{a} = (\bar{X}_i/\bar{X}_M) + (F_i/K_1 y_0)$. Enter the horizontal axis with the value of n_f for the "undamaged" structure, and move parallel to the ξ axis to intersect the solid line with $a = \bar{a}$; n_f' is then read on the 45-degree lines. Alternatively, the reduction factor $\xi_{\bar{a}}$ is used: $n_f' = n_f/\xi_{\bar{a}}$. The penalty is more severe for safer structures.

(ii) The expected number of cycles to failure for systems with limited ductility, n_f''.

Under the designation "limited ductility" a variety of phenomena are collected, which prevent one from taking advantage of the whole force-displacement diagram up to the critical deformation $\bar{X}_M$; collapse occurs when a permanent deformation $|\bar{X}| = |\bar{X}_{MAX}|$ is reached, as shown in Fig. 7. n_f'' is approximately found through the same procedure as n_f', with the only difference that one must consider, within the family of dashed lines in Fig. 6, the one with $b = \bar{X}_{MAX}/\bar{X}_M$. Then: $n_f'' = n_f/\xi_b$. Clearly, one can combine situations (i) and (ii).

(iii) The expected permanent deformation, given the number of response cycles, N.

Let $\bar{n}_f$ be the expected number of cycles to failure, possibly modified as indicated in (i) if the system is initially damaged. Where the line $n_f = \bar{n}_f$ intersects the 45-degree line corresponding to N, the expected permanent deformation is read with reference to the dashed curves. The associated value of b must be interpreted as:

$$b = \begin{cases} E[|\bar{X}|]/\bar{X}_M & \text{if the barriers are initially symmetric,} \\ \dfrac{E[|\bar{X}|] - \bar{a}\,\bar{X}_M}{\bar{X}_M(1 - \bar{a})} & \text{if the system is initially damaged.} \end{cases}$$

The same procedure applies for the case of maximum prescribed ductility; the values of n_f to be used must not include the limitation on $\bar{X}$.

The accuracy of these computations largely depends on the numerical results obtained in Ref. 5. In the range of small stiffness ratios, good agreement was found with simulation results[3]. At the other extreme, as $K_1/|K_2|$ goes to infinity, one has to match the response of elasto-plastic systems[2]; in Fig. 6 this limit behavior was considered to hold also for very small permanent deformations ($\mu \leq 1.03$).

The probability of failure under a motion with given spectral density and duration can also be related approximately to n_f and N. The results in Ref. 5 show that for structures with equal n_f and the same number of response cycles the scatter of the failure probability, P_f, is small. Since P_f slightly increases when the ductility is limited, the chart in Fig. 8 was constructed to give best estimates for $\bar{X}_M/\bar{X}_{MAX} \simeq 3$, and moderately conservative values for larger ductilities. Fig. 8 can be used to find the probability of failure when n_f and N are known (analysis problem), or, reversely, to estimate the required minimum n_f which corresponds to a given probability of failure and to a given earthquake duration (design problem). The value of n_f to be used should be adjusted if either or both conditions (i) and (ii) apply.

ANALYSIS AND DESIGN PROBLEMS

Almost invariably the analysis and design of dynamical systems in a random environment lead to hardly tractable mathematical problems. For the class of hysteretic structures under consideration, the approximate results derived so far allow one to answer some questions in this area, using reasonably simple procedures[6]. In the numerical examples which follow, reference is constantly made to the Kanai-Tajimi spectral density (Eq. 6).

The point we consider first is the sensitivity of the performance to some input and system variations. This is very conveniently done fixing a point in the parameter space, and then making one-dimensional parametric analyses using different variation laws. Studies of this type are helpful to measure the effects of statistical uncertainties in the parameters or to guide a designer's decision.

For usual coefficients of variation the uncertainty in the motion intensity was found to be by far the most important source of stochasticity for the behavior of brittle structures; as the system ductility increases, the probability of failure becomes quite sensitive also to the stiffness ratio. In no case the duration of the motion was a major factor.

Besides direct structural effects, seismic loads may cause widely ranging socio-economic losses. In the judgement of economic damage one usually considers a finite set of deteriorated structural conditions, which, for the class of systems under study, can be defined on the basis of permanent deformation. The stochastic effects of earthquakes are described by a transition matrix, which depends on the model chosen for the seismic environment. We consider here the transition matrix:

(i) conditional to the occurrence of an earthquake motion with given spectral density and duration;

(ii) conditional to the occurrence of a motion with stochastic intensity and duration;

(iii) for a period of time D, during which earthquake occurrence is modeled as a Poisson process and the characteristics of each event are stochastic, as at point (ii).

In the example which follows, a bilinear system with $\omega_n = 2\pi$, $\beta = 0.05$, $y_o = 1$ in., $\bar{X}_M = 40$ in. is subjected to a support acceleration with root mean square: $I = 25$ in/sec^2 and duration: $T = 25$ sec. The damage levels are defined in Table 1. Table 2 collects the expected number of cycles n_{ij} to reach the upper limit of state j, considering as initial permanent deformation the average of the two limits for state i. The transition probabilities (Table 3) are then estimated from Fig. 8, as discussed earlier. When the motion intensity and duration are not deterministic, the transition matrix for a single earthquake is found weighting the transition matrices conditional to given input parameters with the associated probabilities; in the discrete case: $\underline{\pi} = \sum_K p_K \underline{\pi}_K$. The transition matrix for a given period of exposure to seismic risk is a simple elaboration of the previous results when earthquake occurrences follow a Poisson process. In this case damage accumulation is described by a discrete state, continuous time Markov process with transition intensity matrix:

$$\underline{A} = [a_{ij}], \text{ and } a_{ij} = \lambda(P_{ij} - \delta_{ij}),$$

where $1/\lambda$ is the mean interarrival time of events with associated transition matrix $\underline{\pi} = [P_{ij}]$, and δ_{ij} is the Kronecker delta. Then:

$$\underline{\pi}_D = e^{\underline{A}D} = \sum_{n=0}^{\infty} \frac{\underline{A}^n D^n}{n!}$$

The transition matrix in Table 4 refers to the structure defined above, exposed for a period $D = 1/\lambda$ in a seismic zone with the following characteristics:

MOTION	I (in/sec^2)	T (sec)	PROBABILITY
1	20	18	0.70
2	25	25	0.25
3	30	28	0.05

On the line of this procedural scheme, problems of economic analysis can also be studied[6].

Most of the present codes account for seismic action through equivalent static loads, based on the historical local strongest motion, or on the intensity corresponding to a given return period. Unfortunately, it is not easy to find a priori the motion intensity which, for a particular structure, is most critical in terms of expected future loss. For this reason, but even more for establishing a rational aseismic design criterion, the theoretical object should minimize the expected negative utility, the input being defined in probabilistic terms.

To avoid the mathematical difficulties of a full probabilistic approach, the unique optimality condition on the expected utility is replaced by a set of constraints on the system behavior under particular "design motions". The problem is now to find the set of admissible design vectors $\underline{d} = \{\omega_n, \beta, y_o, K_1/|K_2|\}$, among which the optimal choice will be made a posteriori on the basis of utility considerations.

Turning to a specific problem, we want to identify the region of admissible designs, with respect to the following constraints:

MOTION	I (in/sec^2)	T (sec)	P_f	$E[\lvert\bar{X}\rvert]/\bar{X}_M$
1	20	15	$\leq 10^{-4}$	≤ 0.04
2	25	20	$\leq 10^{-2}$	≤ 0.10
3	30	25	$\leq 10^{-1}$	≤ 0.30
4	35	30	≤ 0.3	≤ 0.50

(7)

The computational procedure is discussed in detail in Ref. 6. The design requirements corresponding to each motion are plotted in Figs. 9 and 10 for two representative values of the natural frequency. Prominence is given to the boundary of the admissible region. In this example, the active constraint does not always correspond to the maximum earthquake intensity, emphasizing the necessity of including, in a probability based aseismic design, more than a single performance requirement. The relative importance of the low intensity motions increases with the frequency and with the damping ratio.

When a maximum is imposed to the permanent deformation, the design requirements must be modified. Figs. 11 and 12 compare the results for unlimited ductility (solid lines) with those for a maximum ductility factor $\mu_{MAX} = 21$ (dashed lines). Whenever $K_1/|K_2| \leq 20$, failure occurs for static instability and the design requirements do not change; for higher stiffness ratios the region of admissible points is markedly modified, mainly to balance the reduced hysteretic energy to failure.

We conclude this review of analysis and design problems with some technical considerations. Typically, in technical design, not all the parameters considered previously as "design variables" are in effect controllable. Suppose that the designer is constrained by the following data (units: inches, kips, seconds):

$$m = 4,\ k_2 = -3,\ \beta \text{ non-controllable;}$$

which make the design vector to be a function of K_1 and y_o only: $\underline{d} = \{k_1^{1/2}/2, \beta, y_o, K_1/3\}$. The performance requirements are given in Eq. 7; for simplicity, only the case with unlimited ductility is considered. The solid lines in Fig. 13 give the required minimum yield force f_o as a function of y_o and β; while the elastic stiffness has almost no effect on f_o for large damping ratios, lightly damped stiff systems are safer as compared to soft structures having the same yield force. These requirements are compared with the yield points of actual structures, differing for number of supports, mass height, and column cross section. Particularly interesting is the effect of the height on the system reliability (dashed lines): small variations are of dramatic importance for stiff structures, while, as the system becomes softer and the displacement to yielding increases, the height becomes an unimportant factor.

CONCLUSIONS

An approximate analytic model was used to study the stochastic progression of damage in bilinear systems with negative second slope when exposed to seismic actions. The model provides as main result the expected ductility factor and the probability of failure of any such system when the motion spectral density and duration are specified. "Equivalent" white noise approximations as usually defined for the input were found to give not always accurate results. Parametric analysis has shown that for brittle systems the stochasticity in the response comes mainly from the statistical variability of the motion intensity; the stiffness ratio becomes an important factor for ductile structures. The procedure is also suitable for probabilistic economic analysis and for aseismic design problems where constraints are imposed on the expected ductility factor and on the probability of failure for a finite set of stochastic design motions.

REFERENCES

1. Karnopp, D. and Scharton, T. D., "Plastic Deformation in Random Vibration," J. Acoust. Soc. Amer., Vol. 39, No. 6, 1966.

2. Vanmarcke, E. H. and Yanev, P. I., "Steady State Response of Elasto-Plastic Systems to Random Excitation," XIV South Amer. Conf. on Structural Engineering and IV Pan Amer. Symp. of Structures, Vol. VIII, October 1970.

3. Husid, R., "Gravity Effects on the Earthquake Response of Yielding Structures," Ph.D. Thesis, Cal. Inst. of Technology, Pasadena, California, May 1967.

4. Vanmarcke, E. H. and Veneziano, D., "Probabilistic Seismic Response of Simple Inelastic Systems," Proc. 5WCEE, Rome, Italy, May 1973.

5. Veneziano, D. and Vanmarcke, E. H., "Seismic Damage of Inelastic Systems: a Random Vibration Approach," M.I.T. Dept. of Civil Eng. Research Report R73-5, January 1973.

6. Veneziano, D., "Analysis and Design of Simple Inelastic Structures in a Probabilistic Seismic Environment," M.I.T. Dept. of Civil Eng. Research Report R73-6, January 1973.

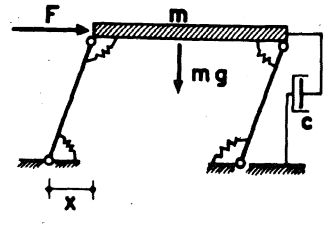

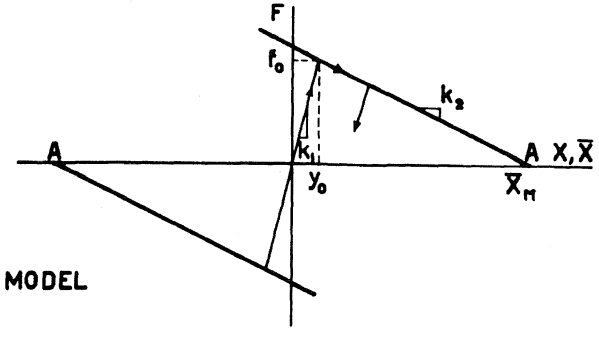

FIG. 1 THE BILINEAR MODEL

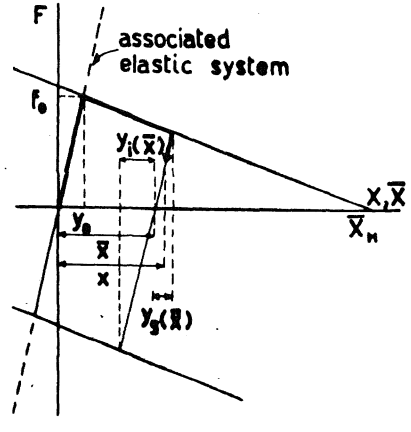

FIG. 2

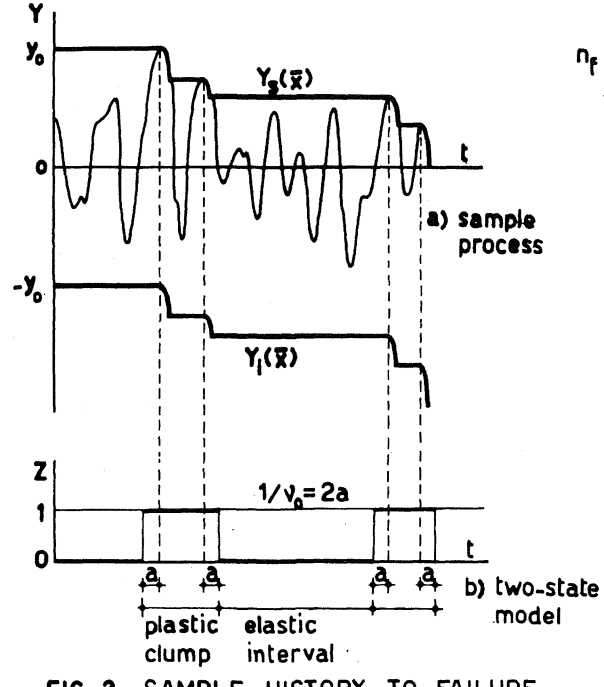

FIG. 3 SAMPLE HISTORY TO FAILURE

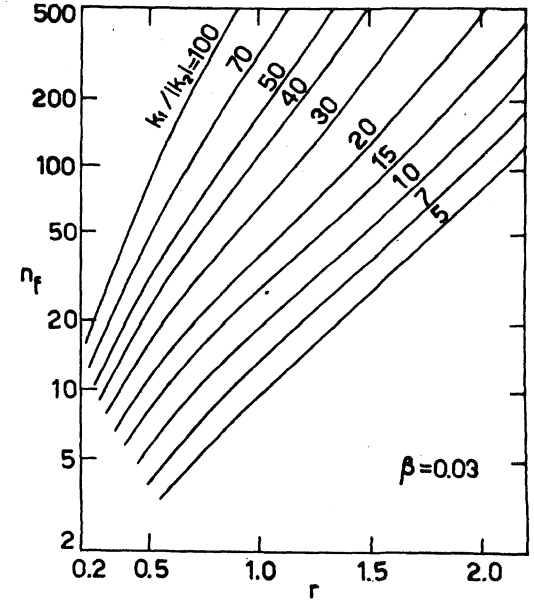

FIG. 4 EXPECTED NUMBER OF CYCLES TO FAILURE

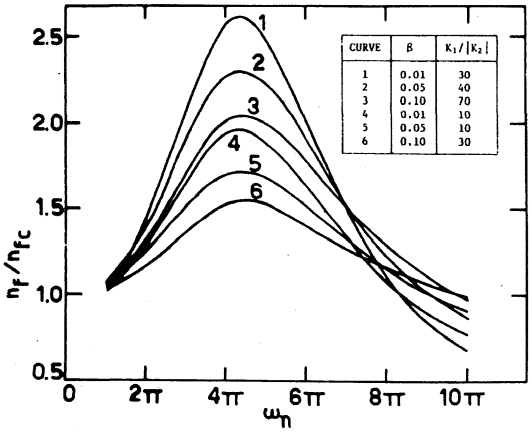

FIG. 5

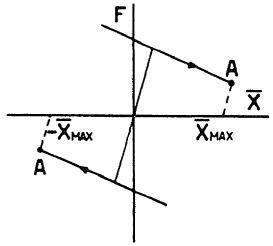

FIG. 7

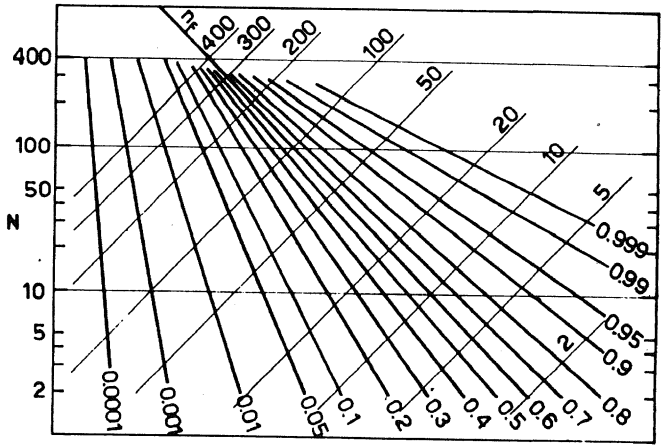

FIG. 8 PROBABILITY OF FAILURE

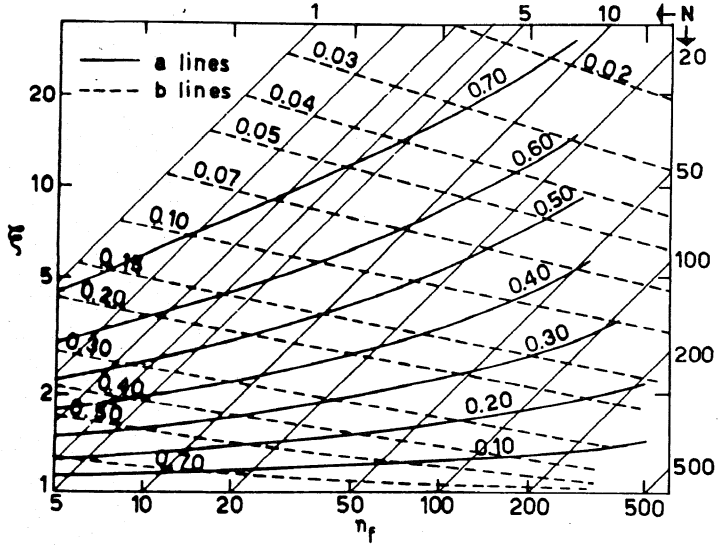

FIG. 6 EXPECTED PERMANENT DEFORMATION

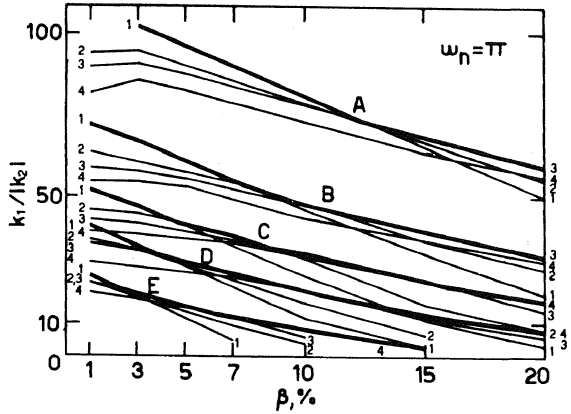

FIG. 9 ADMISSIBLE DESIGN REGIONS

A	y_0 = 1.5 in	D	y_0 = 3.0 in
B	y_0 = 2.0 in	E	y_0 = 4.0 in
C	y_0 = 2.5 in		

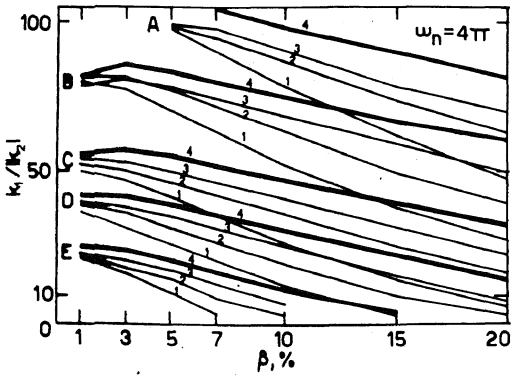

FIG. 10 ADMISSIBLE DESIGN REGIONS
A $y_0=0.25$ in D $y_0=0.50$ in
B $y_0=0.30$ in E $y_0=0.70$ in
C $y_0=0.40$ in

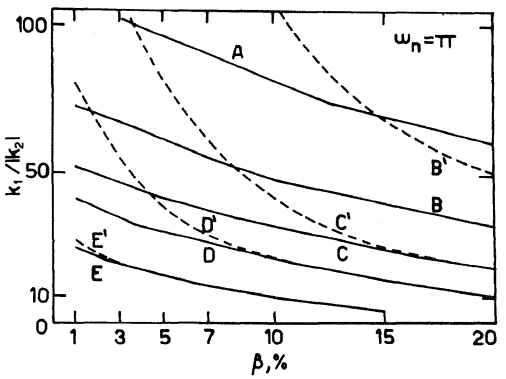

FIG. 11 ADMISSIBLE DESIGN REGIONS
—— unlimited ductility
---- $\mu_{MAX}=21$

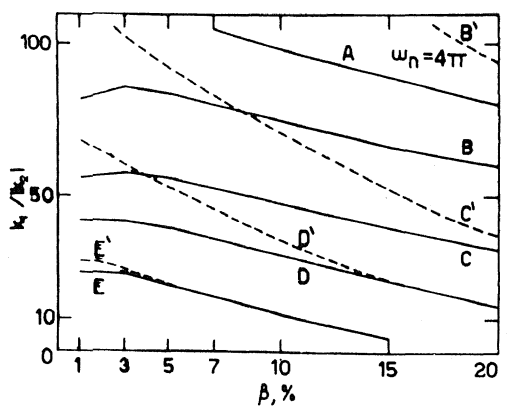

FIG. 12 ADMISSIBLE DESIGN REGIONS
—— unlimited ductility
---- $\mu_{MAX}=21$

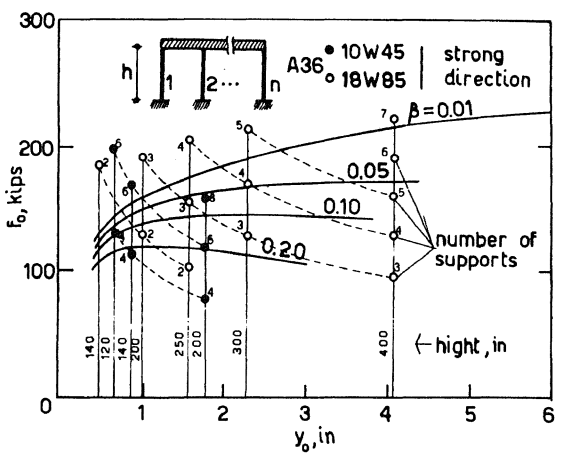

FIG. 13

STATE	NORM. PERM. DEF. $\lvert\bar{x}\rvert/\bar{x}_M$
1	0 : 0.025
2	0.025 : 0.05
3	0.05 : 0.10
4	0.10 : 0.25
5	0.25 : 0.50
6	0.50 : 1

TABLE 1: LEVELS OF DAMAGE

INITIAL STATE	FINAL STATE 1	2	3	4	5
1	2.8	7.2	15.4	36.4	63
2		2.4	10.6	31.6	58.2
3			3.9	24.9	51.5
4				19.9	36.5
5					11

TABLE 2

INITIAL STATE	FINAL STATE 1	2	3	4	5	6
1	0.001	0.024	0.135	0.500	0.240	0.100
2		0.0005	0.0595	0.495	0.320	0.125
3			0.003	0.597	0.220	0.180
4				0.270	0.370	0.360
5					0.100	0.900
6						1

TABLE 3

INITIAL STATE	FINAL STATE 1	2	3	4	5	6
1	0.389	0.126	0.120	0.196	0.088	0.081
2		0.384	0.168	0.247	0.104	0.097
3			0.401	0.362	0.124	0.113
4				0.593	0.223	0.184
5					0.354	0.446
6						1

TABLE 4